

Guiding slow polar molecules with a charged wire

M. Strebels, S. Spieler, F. Stienkemeier, and M. Mudrich*

Physikalisches Institut, Universität Freiburg, D-79104 Freiburg, Germany

(Received 10 August 2011; revised manuscript received 19 October 2011; published 23 November 2011)

We demonstrate experimentally the guiding of cold and slow ND₃ molecules along a thin charged wire over a distance of ~ 0.34 m through an entire molecular beam apparatus. Trajectory simulations confirm that both linear and quadratic high-field-seeking Stark states can be efficiently guided from the beam source up to the detector. A density enhancement up to a factor 7 is reached for beams with velocities ranging down to ~ 150 m/s generated by the rotating nozzle technique.

DOI: [10.1103/PhysRevA.84.053430](https://doi.org/10.1103/PhysRevA.84.053430)

PACS number(s): 37.10.Mn, 37.20.+j, 37.90.+j

I. INTRODUCTION

Considerable experimental effort is directed toward creating dense samples of cold molecules for precision measurements [1], cold chemistry experiments [2–7], quantum information processing [8], and degenerate quantum gases with dipolar interactions [9]. Established techniques for generating velocity-controlled or trapped cold molecules in the temperature range $1 \text{ mK} \lesssim T \lesssim 1 \text{ K}$ include the deceleration using time-varying electric [10], magnetic [11,12], and optical fields [13] and the velocity filtering of polar molecules out of an effusive source using static or time-varying electric fields [14,15]. Alternative routes to producing cold molecules have been demonstrated utilizing the kinematics of elastically or reactively colliding molecular beams [16,17]. Helium nanodroplets are used to prepare molecules and clusters in a cold weakly perturbing environment for spectroscopy and cold chemical reactions studies [18,19]. Ultracold molecules at $T \lesssim 1 \text{ mK}$ can be produced in trapped samples of ultracold atoms via photo- or magneto-association [7,20,21].

A more general and conceptually simple approach to producing slow beams of cold molecules is translating a supersonic jet to low longitudinal velocities by means of a rapidly counter-rotating nozzle. This technique was demonstrated by Gupta and Hershbach [22,23] and recently improved in our group [24]. Using this technique we have demonstrated the production of dense beams of various atomic and molecular species with tunable velocity ranging from ~ 1000 m/s down to $\lesssim 100$ m/s.

Since the molecules are not confined to any external potential this technique suffers from the drawback that beam density rapidly decays due to transverse beam expansion during beam propagation from the nozzle to the interaction region. This effect can be partly compensated by installing additional guiding elements such as an electrostatic quadrupole guide [24]. However, such extended objects cannot easily be brought close to either the nozzle or the interaction region. Besides, electrostatic quadrupole or higher multipole guides produce confining potentials only for molecules in low-field-seeking rotational states. High-field-seeking molecules have been guided and trapped using time-varying electric fields [15,25].

As an alternative guide geometry we use a thin charged wire in this work. The wire is spanned through the whole

molecular beam apparatus from the rotating nozzle up to the quadrupole mass spectrometer (QMS) that we use as a detector. This simple arrangement offers the unique possibility of guiding molecules in high-field-seeking states using electrostatic fields. Even molecules in the rotational ground state can be guided on stable Kepler-like orbits if the electric field is sufficiently high to orient the molecules by “brute force” [26]. This concept was proposed by Sekatskii [27,28] and Loesch [29] and experimentally demonstrated by Loesch and Scheel [30]. Recently, guiding of polar molecules in surface-based electrostatic potentials has been demonstrated [31,32].

In our arrangement we capture the trappable molecules already in the supersonic expansion region and guide them all the way close to the detector. An enhancement of the beam density on the beam axis due to the guiding effect of up to a factor of 7 is measured experimentally for slow beams with velocities $v \lesssim 150$ m/s. Even though the rotational ground state of ND₃ molecules used in our experiment experiences a quadratic Stark effect in the range of applied electric fields, we find from classical trajectory simulations that both ground-state molecules and molecules in rotational states with linear Stark shift can be guided. The guide concept is characterized with regard to optimum geometries and to the applicability to slow molecules in the ground state.

II. EXPERIMENTAL SETUP

The experimental arrangement is identical to the one reported earlier [24] with the difference that the quadrupole guide inserted between skimmer and QMS detector is replaced by a thin wire, as schematically shown in Fig. 1. We use a gold-plated beryllium-copper (BeCu) wire with a radius $R_w = 25 \mu\text{m}$. The total length of the wire from the jet expansion region up to the suspension in front of the detector amounts to 34 cm. The wire is attached at one end to a x - y -translation stage placed inside the source chamber such that the wire can be aligned transversally with respect to the beam axis to pass close by the nozzle ($100 \mu\text{m}$ in diameter) and concentrically through the skimmer. The skimmer aperture has a diameter of 1 mm. Further downstream the wire passes through an intermediate chamber that serves as a differential pumping section. It is suspended inside the detector chamber by a perpendicularly spanned second isolated copper (Cu) wire 15 mm in front of the crossed beam ionizer of the QMS. The BeCu wire is held under tension by a weight of 20 g such that the wire curvature at the point of suspension can be assumed

*marcel.mudrich@physik.uni-freiburg.de

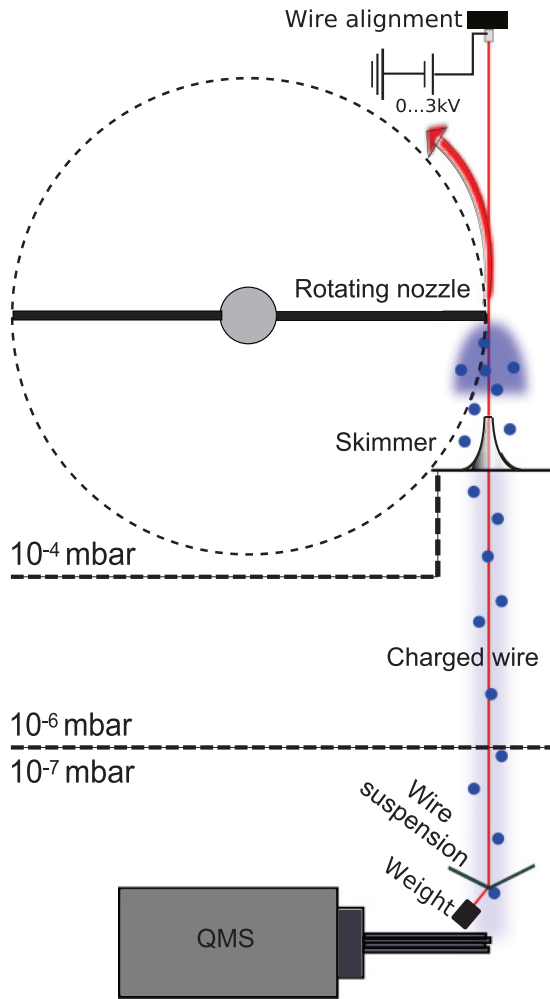


FIG. 1. (Color online) Schematic representation of the experimental setup used for guiding slow polar molecules along a thin charged wire.

to follow the radius of the Cu wire ($50 \mu\text{m}$). Owing to the resulting kink in the electric field a large fraction of the guided molecules are output coupled and enter the detection region of the ionizer of the QMS.

The guide wire is electrically connected to a high-voltage feedthrough inside the source chamber. The maximum applicable voltage is limited to $U \approx 2.2 \text{ kV}$ with respect to the surrounding vacuum chambers by sparkover from the wire either to the skimmer or to the bored titanium ferrule that forms the nozzle at the tip of the rotor arm. Sparking to the skimmer can be prevented by setting the skimmer to high voltage. However, the guide efficiency was found to diminish considerably in this case. Therefore all measurements presented here are performed with the skimmer set to ground potential. In addition, the distance Δx between the center of the nozzle orifice and the wire center is adjusted to $\Delta x \approx 350 \mu\text{m}$ to avoid sparking. This, in turn, means that the nozzle is displaced away from the beam axis by the same distance since the wire is aligned coaxially with the beam axis. As a result, the peak density of the transmitted beam without guide voltage is reduced by about a factor of 4 as compared to the situation when no wire is installed and when the nozzle position is optimized ($\Delta x = 0$).

In the present study we use ND_3 as test molecules to demonstrate the potential of the charged wire setup for guiding slow polar molecules. Since the energy difference between the vibronic ground state $J = 0$ and the lowest rotationally excited states $|J, KM\rangle = |1, \pm 1\rangle$ and $|J, KM\rangle = |1, 0\rangle$ is about 8.3 and 10.3 cm^{-1} , respectively, mostly these states are thermally populated at the estimated low rotational temperatures in the jet of $T \lesssim 10 \text{ K}$. ND_3 is particularly well suited for guiding and deceleration experiments using electric fields due to the strong linear Stark effect of both the high-field-seeking state $|J, KM\rangle = |1, 1\rangle$ and the low-field-seeking state $|J, KM\rangle = |1, -1\rangle$ correlating to the $J = 1$ rotational level which arises from the small inversion splitting in the absence of electric fields [33]. The rovibronic ground state $|0, 0\rangle$ is high-field seeking and features a quadratic Stark effect in the range of field strengths employed in the present work. When placing ND_3 molecules in the electric field of a cylindrical capacitor at a distance r from the center,

$$E(r) = \frac{U}{\ln(R_0/R_w)} \frac{1}{r}, \quad (1)$$

we obtain a transverse trapping potential V that scales as $V(r) \propto r^{-1}$ for the linear Stark state $|1, 1\rangle$ and as $V(r) \propto r^{-2}$ for the ground state $|0, 0\rangle$ [see Fig. 2(a)]. In our setup the electric field is created by a charged wire of radius R_w inside a vacuum apparatus that is assumed to have cylindrical symmetry with inner tube radius $R_0 \sim 20 \text{ mm}$. The shaded area in the center of the figure indicates the range excluded by the wire. While the potential V is attractive for both states in the shown range of distances, V is much deeper ($\sim 1 \text{ cm}^{-1}$) and more extended for the $|1, 1\rangle$ state as compared to the ground

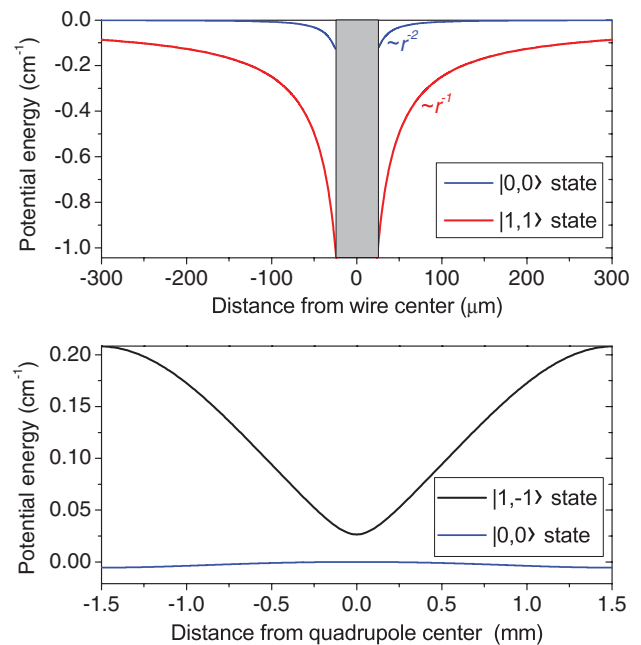


FIG. 2. (Color online) (a) Transverse guide potential of ND_3 molecules in rotational states $|J, KM\rangle = |0, 0\rangle$ (quadratic Stark effect) and $|1, 1\rangle$ (linear Stark effect). A wire diameter of $50 \mu\text{m}$ and an applied voltage $U = 1.5 \text{ kV}$ is assumed. (b) Potential of ND_3 molecules in rotational states $|J, KM\rangle = |1, -1\rangle$ and $|0, 0\rangle$ transverse to the quadrupole electrodes ($U = 1.5 \text{ kV}$).

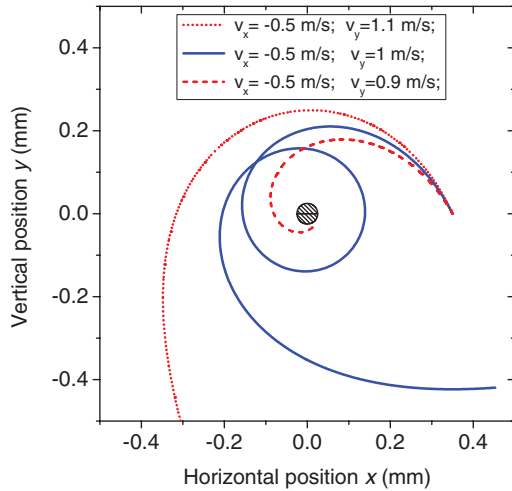


FIG. 3. (Color online) Selected trajectories of ND_3 molecules in the $|0,0\rangle$ ground state propagating in the potential of the wire guide at various values of the initial transverse velocity components v_x and v_y . The longitudinal velocity $v_z = 200$ m/s, the wire voltage $U = 2$ kV, and the distance between the nozzle and the center of the wire, $\Delta x = 350$ μm , are held constant.

state $|0,0\rangle$. Thus, more efficient guiding of molecules in the state $|1,1\rangle$ is expected. Moreover, molecules in $|1,1\rangle$ follow stable elliptical trajectories in analogy to the Kepler problem, whereas the r^{-2} potential experienced by the ground state does not sustain stable trajectories.

For comparison we present in Fig. 2 the transverse potential for ND_3 created by a conventional quadrupole guide as used in our previous work [24]. It consists of four 259-mm-long stainless steel electrode rods, 2 mm in diameter, spaced by a gap of 2 mm between diagonally opposing rods to which a voltage $U = 1.5$ kV is applied. While the ground state $|0,0\rangle$ is subjected to a repulsive potential (light blue line) the state $|1,-1\rangle$ can be transversally bound in a potential well of roughly triangular shape with a depth of about 0.15 cm^{-1} (black line). Thus, the well depth is nearly a factor of 10 lower than the one of the wire guide for the $|1,1\rangle$ state. However, the guide acceptance of the quadrupole is much larger due to the more extended range of the attractive potential of about 3 mm.

Figure 3 displays selected trajectories of ND_3 molecules in the $|0,0\rangle$ ground state traveling in the wire guide at $v_z = 200$ m/s from the nozzle up to the detector plane. Most of the trajectories either spiral downward to hit the wire after a few revolutions (dashed line) or quickly escape away from the wire (dotted line), as discussed in [34]. Only in a narrow range of transverse velocities v_x and v_y are the molecules transiently bound to the wire and reach the detector before crashing into the wire or being expelled away from it (solid line). The corresponding transverse kinetic energies are $E_{\text{kin},\perp} = m(v_x^2 + v_y^2)/2 = 0.9, 1.2, 1.1 \times 10^{-3}$ cm^{-1} , respectively, where m denotes the mass of ND_3 .

The combinations of initial horizontal and vertical transverse velocity components v_x and v_y , respectively, that lead to transiently guided trajectories which end inside the detector area (coaxial circle with radius $R_D = 0.7$ mm) are represented by shaded regions in Figs. 4(a) and 4(b). The semicircular shape of the acceptance of the wire guide in terms of v_x

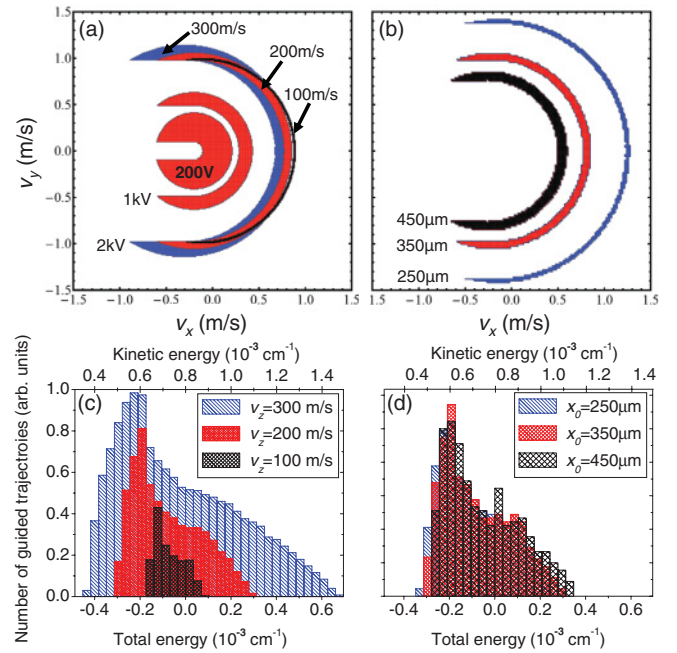


FIG. 4. (Color online) Contour plots illustrating the acceptance of the wire guide for ND_3 molecules in the ground state $|0,0\rangle$ in terms of initial transverse velocity components v_x and v_y : (a) the wire voltage U and the longitudinal velocity v_z are varied at constant $\Delta x = 350$ μm ; (b) the Δx dependence for $U = 2$ kV and $v_z = 200$ m/s. (c) and (d) The corresponding distributions of the total (bottom scale) and kinetic (top scale) energy of the transverse motion.

and v_y reflects the condition for transient guiding. Since all trajectories are asymptotically instable only those with very slow transverse motion $v_{x,y} \lesssim 1$ m/s over the period of propagation to the detector remain in the vicinity of the wire. This is equivalent with the total energy E_{tot} for motion in the x - y plane falling into a narrow interval around zero, $-0.5 \lesssim E_{\text{tot}} \lesssim 0.5 \times 10^{-3}$ cm^{-1} , as depicted by the histograms in Figs. 4(c) and 4(d). Note that the initial potential energy $V_0 = V(r = \Delta x)$ is fixed by the nozzle-wire distance $\Delta x = 350$ μm , which accounts for the shift between E_{tot} and $E_{\text{kin},\perp}$ (top scales). Consequently, the radius of the acceptance semicircle decreases as the potential depth is lowered by lowering the wire voltage from $U = 2$ kV to 200 V at constant longitudinal velocity $v_z = 200$ m/s. In contrast, by varying the beam velocity from $v_z = 100$ to 300 m/s at constant $U = 2$ kV only the width and the position of the semicircular acceptance region are altered. The corresponding E_{tot} distribution [Fig. 4(c)] shrinks both in width and in amplitude as v_z decreases. By varying Δx from 250 to 450 μm for fixed values $U = 2$ kV and $v_z = 200$ m/s, mainly the radius of the acceptance semicircle decreases [Fig. 4(b)] but the E_{tot} distribution changes only marginally [Fig. 4(d)].

Since molecules in the nearly linearly Stark shifted state $|1,1\rangle$ perform Kepler-like trajectories the acceptance for that state is simply defined by the condition $E_{\text{tot}} < 0$ as long as $\Delta x < R_D$. Equivalently, the acceptance region in terms of v_x and v_y is given by a filled circle with radius $\sqrt{2V_0/m} \sim 10$ m/s. Thus, the efficiency of guiding an ensemble of ND_3 molecules produced by a jet expansion is expected to be higher for the molecules in the $|1,1\rangle$ state as compared to those in

the $|0,0\rangle$ by more than a factor of 10, in particular at low longitudinal velocities. Indeed, simulations of the efficiency of guiding beams of ND_3 adapted to the experimental conditions reveal that the measured signal predominantly stems from ND_3 in high-field-seeking states correlating to $J = 1$ and that $|0,0\rangle$ only has a small share in the guiding effect at the applied field strengths, as discussed in the following section. Note that in the experiment performed by Loesch [30] using alkali-halide molecules even the rotational ground states were subjected to a r^{-1} potential due to “brute force” orientation as a result of the much larger dipole moments of the employed molecules and due to higher fields.

III. CHARACTERIZATION OF WIRE-GUIDED BEAMS

The guide efficiency characterized in this section is determined by comparing the detected beam density when switching on the wire voltage U against the density of the unguided beam when the wire potential is set to ground ($U = 0$). Such a measurement using ND_3 (15% seeded in krypton (85%)) for variable beam velocities is depicted in Fig. 5 as open ($U = 0$) and as filled ($U = 2$ kV) symbols. The drop of the absolute density of molecules with decreasing

beam velocity, shown in Fig. 5(a), is due to the transverse and longitudinal dispersion of the beam. This behavior is well reproduced by simple considerations based on the expansion of a bunch of molecules that has Gaussian velocity distributions in longitudinal and transverse directions (dotted line) [24]. Clearly, this drop can be nearly compensated by the wire guide when applying a high voltage U to the wire (filled symbols). Note that guiding is particularly efficient at low velocities in proportion to the unguided beam. The relative density increase due to guiding we call enhancement, which is illustrated in Fig. 5(b). Thus, at beam velocities around 150 m/s we measure an increased beam density by up to a factor of 7. A second measurement was done after the wire was replaced and newly aligned with respect to the nozzle, skimmer, and QMS detector. The two measurements are in good agreement at high beam velocities, whereas at low velocities there are slight deviations probably due to a slightly shifted distance Δx between the nozzle and the wire. Note that the same measurements were also performed using CHF_3 molecules instead of ND_3 . The guide efficiency was found to be very comparable to the one of ND_3 despite the more dense rotational spectrum of CHF_3 .

The solid lines depict the result of classical two-dimensional trajectory simulations for ND_3 which account for the thermal population of all rotational levels $J = 0$ and $J = 1$ at $T = 7$ K as well as for nuclear spin statistics [35]. Initial values for the spatial and velocity coordinates are determined by a Monte Carlo method according to Gaussian velocity distributions and a longitudinal spatial slit opening function of the arrangement determined from fits to the experimental time-of-flight measurements of the unguided beam at various beam velocities [24]. One data point reflects the average of 5000 trajectories bound to the wire potential for each of the 10 rotational states correlating to $J = 0$ and $J = 1$. The two solid lines result from the same simulation and merely reflect the uncertainty in the effective cross section of the ionizer of the QMS. The upper and lower lines correspond to estimated circular cross sections with radius $R_D = 0.5$ mm and $R_D = 0.9$ mm, respectively. Irrespective of this uncertainty, the simulation systematically overestimates the guiding effect by about a factor of 1.5. Possible detrimental effects in the experiment that are not accounted for in the simulation include modulations of the guide potential along the beam axis due to drastically changing outer tube radius R_0 of the assumed cylindrical capacitor configuration, in particular when passing through the skimmer. Furthermore, the incoupling process of the molecules out of the rotating nozzle that sweeps over a range of nozzle-skimmer and nozzle-wire distances Δx as well as the outcoupling mechanism at the wire bend in front of the detector are described in an approximate way.

According to the simulations, the density enhancement by the guiding effect will rise steeply to exceed a factor of 10 as the speed of the molecules is further reduced below $v_z \sim 150$ m/s. However, at such low speeds the beam will be depleted of the molecules in the ground state $|0,0\rangle$ (see Fig. 4 and 11). Unfortunately, we did not reach this velocity range with the present setup due to the limited maximum rotor frequency $\lesssim 300$ Hz [24].

The measured enhancement of the molecule density due to guiding as a function of the wire voltage U for different

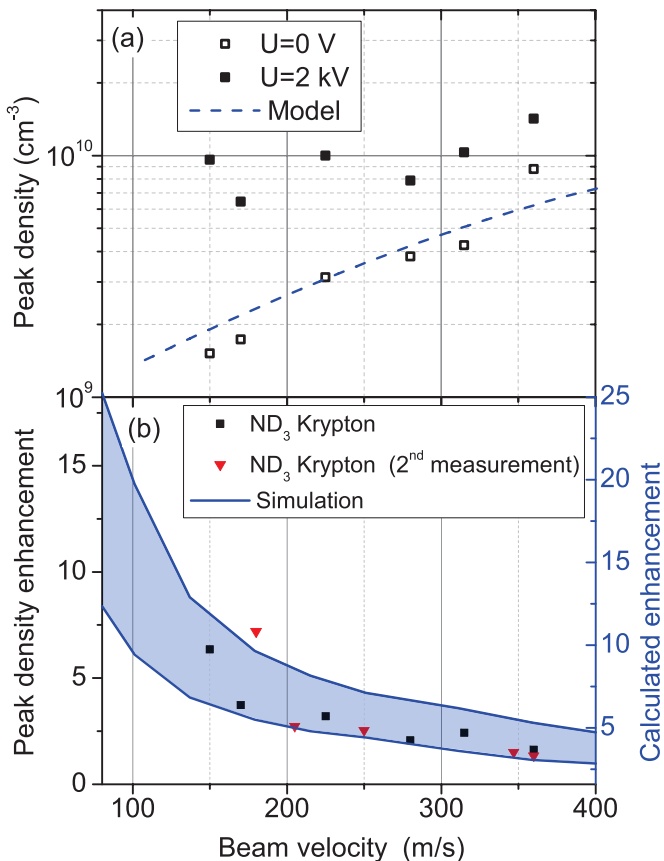


FIG. 5. (Color online) (a) Absolute peak densities of beams of velocity-controlled ND_3 molecules detected behind the wire guide for wire voltage on (2kV) and off (0V). The dashed line represents a model of the free jet expansion based on Gaussian transverse velocity distributions. (b) Relative enhancement of the peak density due to guiding by the charged wire (2kV; left scale). The solid lines show the result of trajectory simulations (see text; right scale).

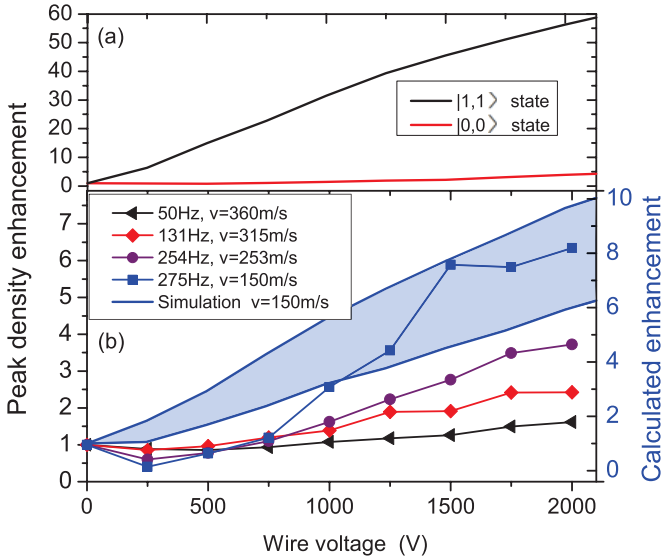


FIG. 6. (Color online) (a) Simulated relative enhancement of the peak density of ND_3 molecules in the high-field-seeking states $|J, KM\rangle = |0,0\rangle$ and $|1,1\rangle$ due to guiding by the charged wire as a function of wire voltage for a beam velocity $v_z = 150$ m/s. (b) Enhancement of the measured ND_3 peak density for various beam velocities (symbols; left scale). The calculations show the average of trajectory simulations for the low-energy Stark states correlating to $J = 0$ and $J = 1$ and for two effective detector cross sections with radius $R_D = 0.5$ mm and $R_D = 0.9$ mm (upper and lower lines, respectively; right scale).

beam velocities v_z is depicted as symbols in Fig. 6(b). As U increases, the number of guided molecules grows monotonically, leading to a relative enhancement factor of up to 7 at $v_z = 150$ m/s. The quadratic Stark state $|0,0\rangle$ contributes much less than the linear Stark state $|1,1\rangle$ in spite of its larger relative population as a consequence of the limited acceptance (see Fig. 2).

The solid lines in Fig. 6(b) depict the results of trajectory simulations for $v_z = 150$ m/s when averaging over all Stark states correlating to $J = 0$ and $J = 1$ according to a thermal distribution. Again, $R_D = 0.5$ mm and $R_D = 0.9$ mm are assumed as lower and upper bounds for the detector radius (upper and lower lines, respectively). Although the trend of a monotonically increasing guide efficiency as a function of U as well as the magnitude of the effect are both reasonably well reproduced, the simulation slightly deviates from the measurement at low voltages. This is presumably due to the simplified description of the experimental setup that we have employed in the simulations, as mentioned above. Possibly, also the Stark state $|0,0\rangle$, which shows a similar voltage dependence as the experimental data [see Fig. 6(a)], has a larger share in the experimental signal than assumed in the simulations.

It is instructive to compare the performance of the charged wire guide with a conventional linear quadrupole guide in terms of guide efficiency. To this end, we present in Fig. 7 the density enhancement measured with a beam of ND_3 molecules injected into a quadrupole guide as used previously [24]. The guide is implemented in our setup between the skimmer and the ionizer of the QMS. In this arrangement the beam path can

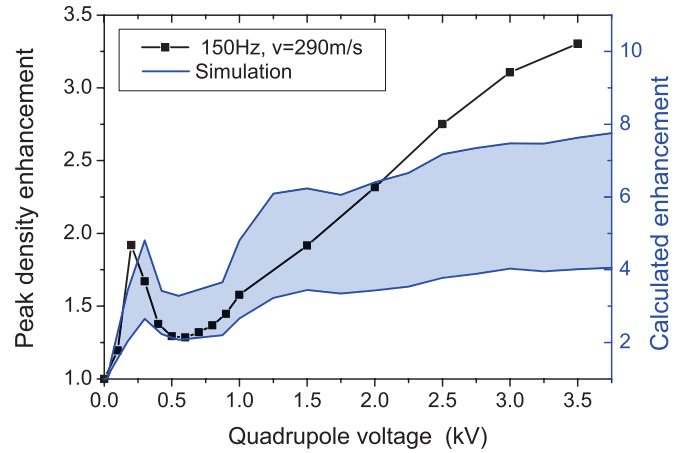


FIG. 7. (Color online) (b) Relative enhancement of the measured ND_3 peak density due to guiding in a linear quadrupole for a beam velocity $v_z = 290$ m/s as a function of the applied voltage (left scale). The calculations show the results of trajectory simulations for two effective detector cross sections with radius $R_D = 0.5$ mm and $R_D = 0.9$ mm (upper and lower lines, respectively; right scale).

be divided into three segments: free flight from the nozzle to the entrance of the quadrupole guide right behind the skimmer, bound or unbound trajectories inside the quadrupole guide, and again free flight from the exit of the guide up to the detector. In spite of the additional free flight region between the nozzle and the entrance of the quadrupole guide, we find very similar guide efficiencies for both types of guides for the same beam velocities (factor of 2–3). This is due to the larger phase-space acceptance of the quadrupole guide as compared to the wire guide in spite of the lower depth of the guide potential well. The initial maximum at low voltages in Fig. 7 is due to oscillatory trajectories inside the anharmonic guide potential, which lead to a focusing of the molecules onto the beam axis after the first half-period of the oscillation [24].

The dependence of the enhancement factor on the distance Δx between the center of the charged wire and the nozzle orifice is shown in Fig. 8. In this measurement, the wire voltage is set to a moderate value $U = 1.5$ kV to avoid sparking, the beam velocity is held constant at $v_z = 310$ m/s, and the distance between the wire and nozzle is varied from $500 \mu\text{m}$ to the minimum distance of about $350 \mu\text{m}$. This is achieved by shifting the whole baseplate that supports the rotating nozzle setup with respect to the position of the charged wire which is kept fixed. In this way, the geometry of the guiding field and of the detector is kept unchanged during the measurement. Note that the nozzle to wire distance is determined by viewing the nozzle position through a telescope along the wire axis. Therefore the value of Δx must be regarded as an estimate with an absolute uncertainty of about $50 \mu\text{m}$.

Clearly, as the nozzle is brought as close as possible to the charged wire the guide efficiency slightly increases by up to a factor of about 2. This is due to the increased depth of the guide potential close to the wire surface such that a larger fraction of molecules with nonvanishing transverse velocity components still remain bound to the wire potential. At the same time, the absolute signal of the unguided beam is increased by a factor of 1.5 since the nozzle is moved toward the beam axis, as

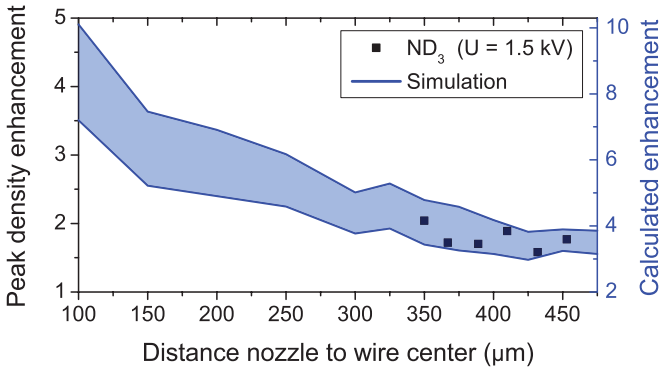


FIG. 8. (Color online) Measured (symbols; left scale) and simulated (lines; right scale) enhancement of the ND_3 peak density due to guiding by the charged wire as a function of the distance Δx between the center of the nozzle orifice and the center of the wire. The beam velocity and wire voltage are fixed to $v_z = 310$ m/s and $U = 1.5$ kV, respectively.

mentioned above. The trajectory simulations for $R_D = 0.5$ mm and $R_D = 0.9$ mm (solid lines) reproduce this trend but again clearly overestimate the overall enhancement. By further decreasing the distance, the enhancement could be increased by an additional factor of about 2 according to the simulation.

Since the electric field, which is generated by applying a certain voltage U to the wire, depends on the wire radius R_w according to Eq. (1) as shown in Fig. 9(a), the choice of R_w crucially influences the guide efficiency. In order to determine the optimum value of R_w for the given conditions in our experiment we have performed simulations of the density enhancement for ND_3 at $U = 1.5$ kV and $v_z = 310$ m/s for various values of R_w ranging from 90 to $0.5 \mu\text{m}$ [Fig. 9(b)]. The two lines for either $|0,0\rangle$ and $|1,1\rangle$ states represent the results for $\Delta x = 375 \mu\text{m}$ and $\Delta x = 475 \mu\text{m}$. As R_w is reduced to $\sim 10 \mu\text{m}$ the guide efficiency first rises in spite of the decreasing electric field [Fig. 9(a)] due to an increased number of trajectories that circle around the wire without hitting it. A clear maximum occurs around $10 \mu\text{m}$, corresponding to an optimum guide efficiency for molecules in the $|1,1\rangle$ state. For smaller values of $R_w \lesssim 10 \mu\text{m}$, the guide efficiency goes down again due to a sharp drop of the electric field. However, for practical reasons, such as stability against tensile stress and electric sparkover, we chose the BeCu wire with $50 \mu\text{m}$ diameter.

The simulated enhancement of the ND_3 beam density as a function of the tube radius R_0 is shown in Fig. 10(b) for molecules in the rotational states $|0,0\rangle$ and $|1,1\rangle$. In this simulation a wire voltage of $U = 1.5$ kV and a beam velocity of $v_z = 310$ m/s are assumed, while the nozzle to wire distance is held constant at $\Delta x = 375 \mu\text{m}$. As the tube radius is reduced from 150 mm to about $500 \mu\text{m}$ the guide efficiency rises continuously due to the monotonic increase of the electric field according to Eq. (1) as shown in Fig. 10(a). By implementing an additional tube electrode with 1 mm in diameter the guide efficiency in our setup could theoretically be enhanced by nearly a factor of 2. Due to technical difficulties such as the passage through the skimmer and the outcoupling of the molecules at the wire suspension, however, we abandoned the option of using an outer tube.

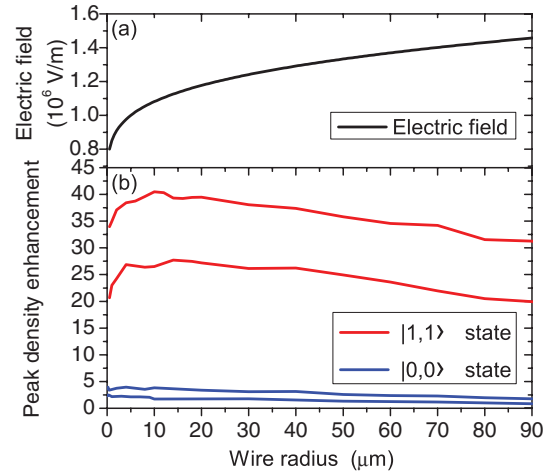


FIG. 9. (Color online) (a) Electric field according to Eq. (1) at a distance $\Delta x = 375 \mu\text{m}$ from the wire center as a function of the wire radius. (b) Simulated behavior of the ND_3 peak density due to guiding by the charged wire as a function of the wire radius for $\Delta x = 375 \mu\text{m}$ and $\Delta x = 475 \mu\text{m}$ (upper and lower lines, respectively). The beam velocity and the wire voltage are fixed to $v_z = 310$ m/s and $U = 1.5$ kV, respectively.

The simulations presented so far show that ND_3 in both the linear $|1,1\rangle$ and the quadratic Stark state $|0,0\rangle$ can be guided along the charged wire in spite of the trajectories in a r^{-2} potential being unstable. Therefore the question arises as to under which conditions this instability becomes apparent as reduced guide efficiency. In order to illustrate this effect we simulate the enhancement of the density of ND_3 molecules in the ground state $|0,0\rangle$ for beam velocities reaching down to $v_z \sim 20$ m/s (Fig. 11). The wire voltage $U = 1.5$ kV, the nozzle position $\Delta x = 350 \mu\text{m}$, and the wire radius are held constant. As the velocity is decreased from $v_z = 400$ m/s to $v_z = 100$ m/s the density enhancement first rises similarly to the state-averaged density shown in Fig. 5. However, at lower beam velocities $v_z < 100$ m/s the guiding effect sharply

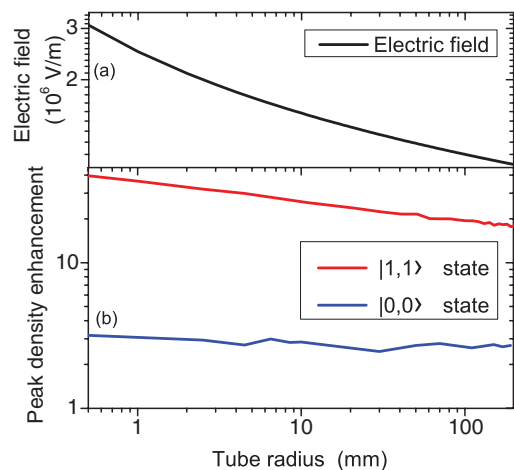


FIG. 10. (Color online) (a) Electric field according to Eq. (1) at $\Delta x = 375 \mu\text{m}$ as a function of the tube radius. (b) Simulated enhancement of the ND_3 peak density as a function of the tube radius. The beam velocity and the wire voltage are fixed to $v_z = 310$ m/s and $U = 1.5$ kV, respectively.

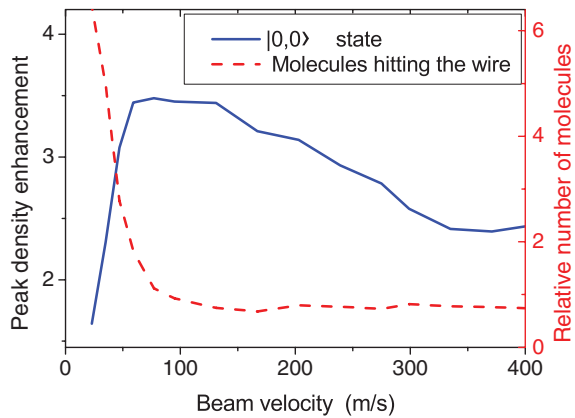


FIG. 11. (Color online) Simulated density enhancement of ND_3 molecules in the ground state $|0,0\rangle$ as a function of velocity down to $v_z \sim 20$ m/s (solid line; left scale). The dashed line indicates the number of molecules that hit the wire on their way from the nozzle to the detector in proportion to the number of detected molecules (right scale).

breaks down due to an increasing fraction of molecules that impinge onto the wire (dashed line). As the wire radius is further reduced, the position of the maximum slightly shifts downward to lower velocities. We conclude that under the present conditions of a quadratically Stark shifted ground state the charged wire may only be useful for guiding ground-state molecules at moderate velocities in the range of hundreds of meters per second, whereas it is inapplicable for molecules decelerated well below $v_z \sim 100$ m/s. When applying higher voltages and using molecules with larger dipole moments, however, even ground-state molecules would be subjected to the linear Stark effect and could consequently be guided along stable trajectories with similar efficiencies as the molecules in higher high-field-seeking rotational states.

IV. SUMMARY AND OUTLOOK

In conclusion, we have demonstrated that a simple, thin charged wire placed along the axis of a beam of slow polar ND_3 molecules can be used for enhancing the molecule

density even at the exit of the wire guide by up to a factor of 7. Simple classical trajectory simulations are found to reproduce the systematic trends and the overall magnitude of the effect up to a factor 1.5. While rotational states with linear Stark effect are guided along the wire in stable Kepler-like orbits, the ground state, which is quadratically Stark shifted at the electric fields applied in our setup, is only slightly enhanced at moderate beam velocities due to transient guiding along asymptotically unstable trajectories. Possible technical improvements of the present setup include higher wire voltages up to $U \gtrsim 3$ kV, which could be reached by insulating the tip of the rotor against the vacuum apparatus to suppress sparking. Additionally, the skimmer aperture could be enlarged when using an additional differential pumping section. Then, even ground-state molecules could be efficiently guided on stable orbits. Furthermore, a new nozzle design will feature a thinned end cap of the titanium ferrule in order to reduce the distance between the nozzle orifice and the wire surface to ~ 100 μm . In this way both the guide efficiency with respect to $U = 0$ is enhanced and the absolute beam intensity is increased due to better beam alignment. In total, higher peak densities by about a factor of $\gtrsim 5$ as compared to the reported guided beam densities should be attainable.

Several applications of the presented concept are conceivable. Since only polar molecules experience the electrostatic guiding force, in contrast to the rare-gas atoms in the carrier gas of the seeded expansion, such a guiding element can be used to separate the molecules out of the carrier gas beam, in particular if an additional bend section is incorporated. The implementation of a wire guide into novel intense sources of cold molecules that rely on buffer gas cooling in combination with expansion cooling may be promising [36,37]. Such an approach may be particularly advantageous in applications where cold molecules are to be injected into microstructured devices such as microcavities or atom chips.

ACKNOWLEDGMENTS

We thank H. J. Loesch for stimulating discussions. We are grateful for support by the Landesstiftung Baden-Württemberg as well as by DFG.

-
- [1] J. J. Hudson, B. E. Sauer, M. R. Tarbutt, and E. A. Hinds, *Phys. Rev. Lett.* **89**, 023003 (2002).
- [2] P. F. Weck and N. Balakrishnan, *Int. Rev. Phys. Chem.* **25**, 283 (2006).
- [3] E. Bodo, F. A. Gianturco, N. Balakrishnan, and A. Dalgarno, *J. Phys. B* **37**, 3641 (2004).
- [4] S. Willitsch, M. T. Bell, A. D. Gingell, S. R. Procter, and T. P. Softley, *Phys. Rev. Lett.* **100**, 043203 (2008).
- [5] I. W. Smith, *Low Temperatures and Cold Molecules* (Imperial College Press, London, 2008).
- [6] R. V. Krems, *Int. Rev. Phys. Chem.* **24**, 99 (2005).
- [7] R. Krems, B. Friedrich, and W. Stwalley, *Cold Molecules* (CRC Press, Boca Raton, 2009).
- [8] D. DeMille, *Phys. Rev. Lett.* **88**, 067901 (2002).
- [9] M. Baranov *et al.*, *Phys. Scr.*, **T 102**, 74 (2002).
- [10] H. I. Bethlem, G. Berden, and G. Meijer, *Phys. Rev. Lett.* **83**, 1558 (1999).
- [11] S. D. Hogan, D. Sprecher, M. Andrist, N. Vanhaecke, and F. Merkt, *Phys. Rev. A* **76**, 023412 (2007).
- [12] E. Narevicius, A. Libson, C. G. Parthey, I. Chavez, J. Narevicius, U. Even, and M. G. Raizen, *Phys. Rev. Lett.* **100**, 093003 (2008).
- [13] R. Fulton, A. Bishop, M. Shneider, and P. Barker, *Nature Phys.* **2**, 465 (2006).
- [14] S. A. Rangwala, T. Junglen, T. Rieger, P. W. H. Pinkse, and G. Rempe, *Phys. Rev. A* **67**, 043406 (2003).
- [15] T. Junglen, T. Rieger, S. A. Rangwala, P. W. H. Pinkse, and G. Rempe, *Phys. Rev. Lett.* **92**, 223001 (2004).

- [16] M. S. Elioff, J. J. Valentini, and D. W. Chandler, *Science* **302**, 1940 (2003).
- [17] N.-N. Liu and H. Loesch, *Phys. Rev. Lett.* **98**, 103002 (2007).
- [18] M. Mudrich, O. Bünermann, F. Stienkemeier, O. Dulieu, and M. Weidemüller, *Eur. Phys. J. D* **31**, 291 (2004).
- [19] S. Müller, S. Krapf, Th. Koslowski, M. Mudrich, and F. Stienkemeier, *Phys. Rev. Lett.* **102**, 183401 (2009).
- [20] K. M. Jones, E. Tiesinga, P. D. Lett, and P. S. Julienne, *Rev. Mod. Phys.* **78**, 483 (2006).
- [21] C. Chin, R. Grimm, P. Julienne, and E. Tiesinga, *Rev. Mod. Phys.* **82**, 1225 (2010).
- [22] M. Gupta and D. Herschbach, *J. Phys. Chem. A* **103**, 10670 (1999).
- [23] M. Gupta and D. Herschbach, *J. Phys. Chem. A* **105**, 1626 (2001).
- [24] M. Strebel, F. Stienkemeier, and M. Mudrich, *Phys. Rev. A* **81**, 033409 (2010).
- [25] M. Schnell, P. Lützwow, J. van Veldhoven, H. L. Bethlem, J. Küpper, B. Friedrich, M. Schleier-Smith, H. Haak, and G. Meijer, *J. Phys. Chem. A* **111**, 7411 (2007).
- [26] H. J. Loesch, *Annu. Rev. Phys. Chem.* **46**, 555 (1995).
- [27] S. K. Sekatskii, *Pis'ma Zh. Éksp. Teor. Fiz.* **62**, 900 (1995) [*JETP Lett.* **62**, 916 (1995)].
- [28] S. K. Sekatskii and J. Schmiedmayer, *Europhys. Lett.* **36**, 407 (1996).
- [29] H. J. Loesch, *Chem. Phys.* **207**, 427 (1996).
- [30] H. J. Loesch and B. Scheel, *Phys. Rev. Lett.* **85**, 2709 (2000).
- [31] Y. Xia, Y. Yin, H. Chen, L. Deng, and J. Yin, *Phys. Rev. Lett.* **100**, 043003 (2008).
- [32] L. Deng, Y. Liang, Z. Gu, S. Hou, S. Li, Y. Xia, and J. Yin, *Phys. Rev. Lett.* **106**, 140401 (2011).
- [33] H. L. Bethlem, G. Berden, F. M. H. Crompvoets, R. T. Jongma, A. J. A. van Roij, and G. Meijer, *Nature (London)* **406**, 491 (2000).
- [34] J. Denschlag, G. Umshaus, and J. Schmiedmayer, *Phys. Rev. Lett.* **81**, 737 (1998).
- [35] C. H. Townes and A. L. Schawlow, *Microwave Spectroscopy, Volume 1* (McGraw-Hill, New York, 1955).
- [36] H.-I. Lu, J. Rasmussen, M. J. Wright, D. Patterson, and J. M. Doyle, *Phys. Chem. Chem. Phys.* **13**, 18986 (2011).
- [37] N. R. Hutzler, M. F. Parsons, Y. V. Gurevich, P. W. Hess, E. Petrik, B. Spaun, A. C. Vutha, D. DeMille, G. Gabrielse, and J. M. Doyle, *Phys. Chem. Chem. Phys.* **13**, 18976 (2011).